

## CFRP Strengthening of Rectangular Steel Tubes Subjected to End Bearing Loads: Effect of Adhesive Properties

D. Fernando<sup>1</sup>, T. Yu<sup>1</sup>, J.G. Teng<sup>1</sup>, and X.L. Zhao<sup>2</sup>

<sup>1</sup> Department of Civil and Structural Engineering  
The Hong Kong Polytechnic University, Hong Kong, China

<sup>2</sup> Department of Civil Engineering  
Monash University, Clayton, VIC 3168, Australia

**ABSTRACT:** The end bearing capacity of a rectangular hollow section (RHS) steel tube can be substantially increased through local strengthening using bonded FRP plates. As failure of such a strengthened tube generally occurs by debonding of the FRP plates from the steel tube, the effectiveness of such strengthening depends significantly on the properties of the adhesive. This paper presents the results of an experimental study aimed at clarifying the effects of adhesive properties on the failure mode and the load-carrying capacity. The experimental programme included sixteen tests covering five different commercially available adhesives. Four different failure modes were observed in these tests: (1) adhesion failure; (2) cohesion failure; (3) combined adhesion and cohesion failure; (4) interlaminar failure of CFRP plates. The tests also revealed that an adhesive with a larger ultimate tensile strain leads to a greater load-carrying capacity of the strengthened RHS tube.

**KEYWORDS:** RHS, steel tubes, CFRP, strengthening, end bearing, adhesives.

### 1. INTRODUCTION

Web crippling under transverse bearing is a common failure mode of thin-walled steel sections and has been studied by many researchers (e.g. Packer 1984, 1987; Zhao and Hancock 1992, 1995). Zhao *et al.* (2006) recently explored the use of bonded CFRP plates to enhance the transverse end bearing load capacity of steel rectangular hollow section (RHS) tubes through a series of tests. These tests showed that bonding of CFRP plates provides an effective means of enhancing the end bearing load capacity of RHS tubes. These tests also revealed that debonding of the CFRP plates from the steel substrate is a common phenomenon in such CFRP-strengthened RHS tubes.

Debonding failure is always a concern for hybrid structures where two or more materials are bonded together using adhesives. Extensive research has been conducted on debonding failures in FRP-strengthened concrete structures (Smith and Teng 2002; Teng *et al.* 2002) but much less is known about debonding failures in FRP-strengthened steel structures (Hollaway and Cadei 2002; Zhao and Zhang 2007). Debonding failures in FRP-strengthened concrete structures generally occur in the concrete which is the weakest link of the system, but debonding failures in FRP-strengthened steel structures generally occur within the adhesive (cohesion failure) or at the physical interfaces between the adhesive and the adherends (adhesion failure) (Schnerch 2005; Xia and Teng 2008). In addition, a combination of adhesion failure and cohesion failure (i.e. combined adhesion and cohesion failure) may occur (Schnerch 2005). A cohesion failure is completely controlled by the properties of the adhesive while an adhesion failure depends also on the surface characteristics of the adherends including the texture, roughness and chemical composition of the surface (Schnerch 2005). To fully understand the bond behaviour of adhesively-bonded joints between FRP and steel, both the effects of adhesive properties and surface characteristics of adherends need to be clarified. This paper presents the results of an experimental study on the effects of adhesive properties on the failure mode and load-carrying capacity of CFRP-strengthened RHS tubes subjected to end bearing loads.

## 2. EXPERIMENTAL PROGRAMME

In the present study, sixteen specimens were tested under end bearing loads. These specimens included one bare RHS tube as the reference specimen (Figure 1a) and fifteen CFRP-strengthened RHS tubes (Figure 1b); five different adhesives were used to bond the CFRP plates and three identical specimens were made using each adhesive. The five adhesives (referred to as adhesives A to E) are commonly available in the market and were chosen to cover a wide range of material properties. For ease of reference, the name of each specimen starts with a letter that represents the adhesive, followed by a Roman number to differentiate the three nominally identical specimens with the same adhesive. For each of the CFRP-strengthened RHS tubes, CFRP plates were bonded to the outer surfaces of the two webs, as shown in Figure 1(b). This strengthening scheme was found by Zhao *et al.* (2006) to be highly effective. All specimens were made from identical steel tubes and high-modulus CFRP plates. The CFRP plates were cut to a size of 92 mm in length and 50 mm in width and two such plates were bonded to each web. The specimen details are summarized in Table 1 while the properties of the steel and the CFRP are given in Table 2. The material properties of the CFRP are those supplied by the manufacturer. The material properties of the steel were found from tensile coupon tests; coupons cut from both the flat regions and the corners of the steel tube were tested as their properties were expected to be different. Coupon tests were also conducted to obtain the tensile properties of the five adhesives used in this study. Five coupons were tested for each adhesive. The key results averaged from the five coupon tests for each adhesive are given in Table 3 and typical stress-strain curves of these adhesives are shown in Figure 2. It is evident from Table 3 that the five adhesives cover a wide range of elastic modulus (from 1.8 GPa to 11 GPa) and ultimate tensile strain (from 0.003 to 0.0289).

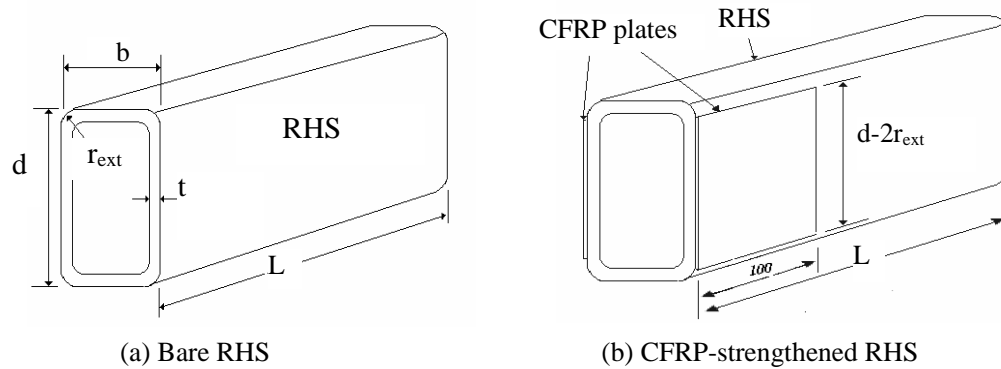


Figure 1. Bare and CFRP-strengthened RHS tubes

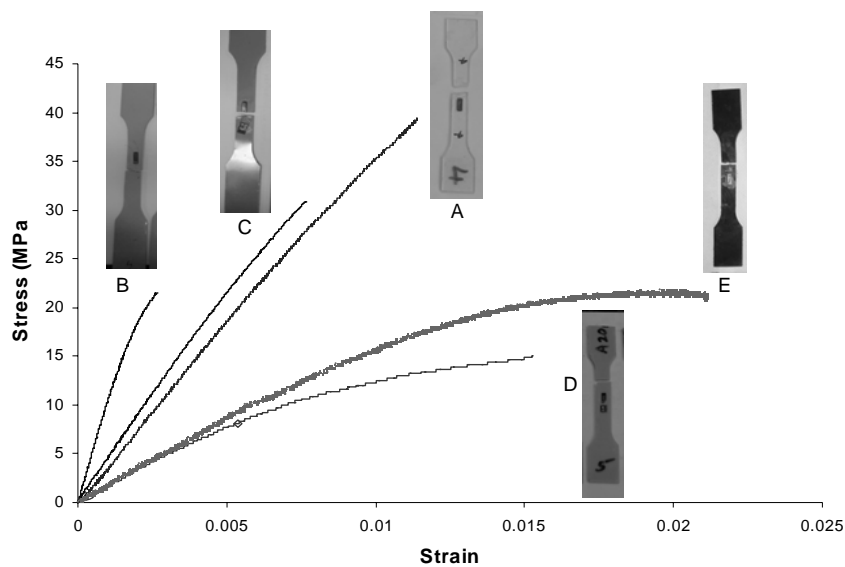


Figure 2. Tensile stress-strain curves of different adhesives

Based on the guidelines proposed by Schnerch (2005), the following procedure was adopted in preparing the CFRP-strengthened specimens. The outer web surfaces of a steel tube were first grit-blasted using 0.5mm angular grit. The CFRP plates were then bonded to the prepared surfaces within 24 hours. The adhesive layer was designed to be 1 mm thick and this thickness was closely controlled using glass spacers except when adhesive A was used. For the latter, a uniform thickness was difficult to achieve despite the use of glass spacers because of the low viscosity of the adhesive. This poor control of the adhesive thickness was expected to lead to inferior bond performance.

All the end bearing tests were conducted using a 2000 kN capacity Forney universal testing machine with load control at a loading rate of approximately 2 kN per minute. A schematic view of the test set-up is shown in Figure 3.

Table 1. Specimen details

	Height, d (mm)	Width, b (mm)	Thickness, t (mm)	Length, L (mm)	Bearing length (mm)
RHS	99.8	50.1	1.78	202	50
CFRP	92	N/A	1.4	100	N/A

Table 2. Material properties of CFRP and steel

		E, (GPa)	$\sigma_{0.2}$ , (MPa)	$\sigma_u$ (MPa)
RHS	Flats	192	322	370
	Corners	198	390	450
CFRP		300	N/A	1300

Table 3. Material properties of adhesive

Adhesive	Modulus of elasticity, E (MPa)	Ultimate stress, $f_u$ (MPa)	Ultimate strain, $\epsilon_u$
A	3975	40.7	0.0111
B	11250	22.3	0.0030
C	4820	31.3	0.0075
D	1750	14.7	0.0151
E	1828	21.5	0.0289

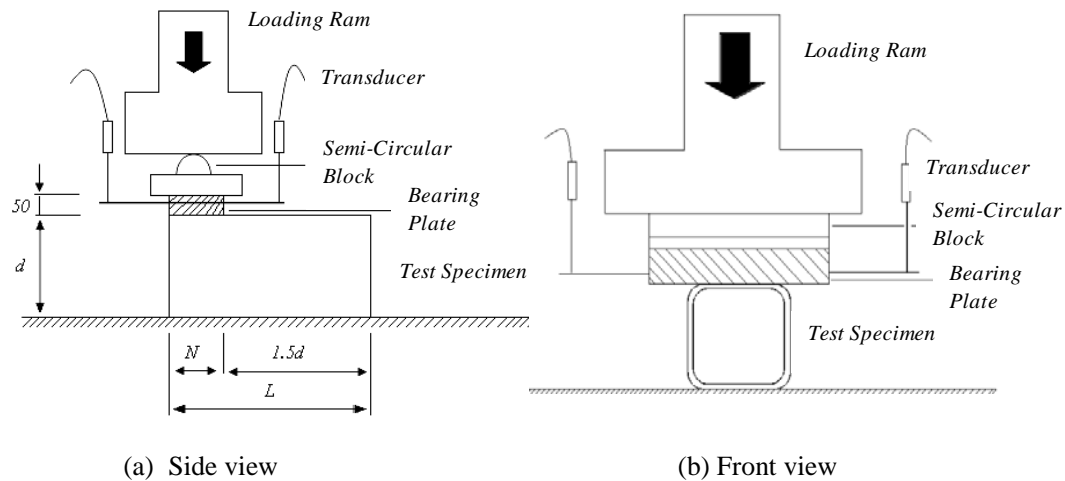
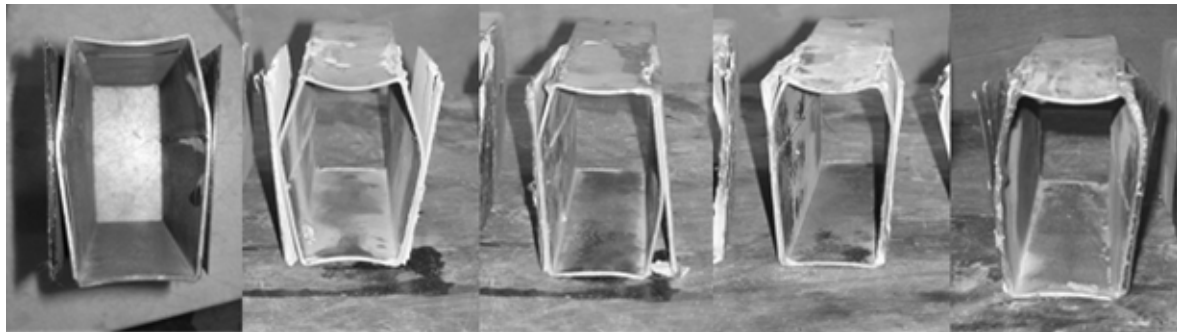


Figure 3. Schematic view of the test set-up

### 3. RESULTS AND DISCUSSIONS

The failed specimens are shown in Figure 4 and the key test results are summarized in Table 4. Except for the specimens with adhesive E, failure occurred by the debonding of the CFRP plates followed by web buckling; a number of different debonding failure modes were observed. Adhesion failure at the steel/adhesive interface occurred in specimens with adhesive A, cohesion failure occurred in specimens with adhesive B, while combined adhesion (at the steel/adhesive interface) and cohesion failure was found in specimens with adhesives C and D. Specimens with adhesive E failed by the interlaminar failure of the CFRP plates (referred to as “CFRP failure” hereafter) again followed by web buckling.



(a) Adhesive A (b) Adhesive B (c) Adhesive C (d) Adhesive D (e) Adhesive E  
Figure 4. Specimens after testing

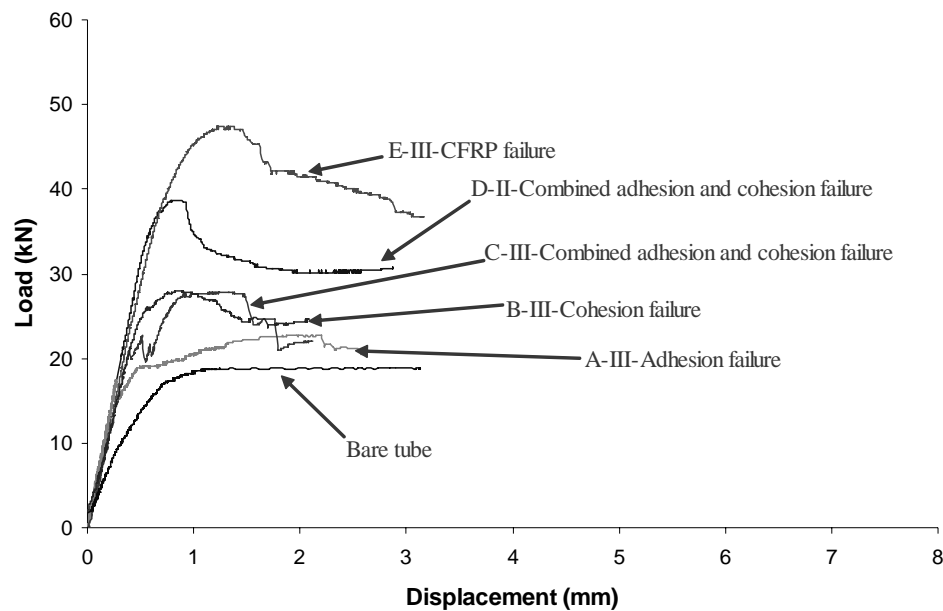


Figure 5. Load-displacement curves of bare and CFRP-strengthened steel tubes

Typical load-deflection curves are shown in Figure 5. It is evident from Figure 5 that all the CFRP-strengthened RHS tubes had almost the same initial stiffness despite the use of different adhesives and this initial stiffness is much higher than that of the bare RHS tube. These results indicate that the different adhesives were all able to mobilise the contribution of the CFRP plates in the initial stage of loading and their different elastic moduli had little effect on the overall stiffness of the strengthened specimens.

Debonding of the CFRP plates always initiated from one of the plate ends, but the propagation of debonding differed for different adhesives. In specimens B (i.e. specimens with adhesive B) and C, debonding propagated gradually towards the mid-height of the web after the appearance of the first crack at the plate end; the load kept increasing during this process (Figure 5). By contrast, in specimens D, debonding was more localized near the plate end and its propagation was rapid; the load dropped immediately after cracking was noted near the plate end (Figure 5). Formation of plastic hinges always

followed debonding and these plastic hinges were always located at the end of the debonded region. The lateral deflection of the web increased rapidly after first cracking as a result of the loss of the resistance offered by the CFRP plates against web buckling. The initial cracking at the plate end is believed to be caused by high interfacial stresses (i.e. shear and normal stresses) developed in this region; similar interfacial stress concentrations in FRP-strengthened concrete beams have been extensively studied (e.g. Smith and Teng 2002). For specimens B and C where the first crack happened at a relatively low load level, an increasing load could be resisted without web buckling following initial cracking so the debonding process was gradual. For specimens D, the web was unable to resist the applied load after initial cracking so debonding was sudden and the load dropped immediately.

Table 4 and Figures 4 and 5 show that the adhesive properties significantly affected the behaviour of CFRP-strengthened RHS tubes under end bearing loads. Obviously, the failure modes of the specimens depended significantly on the adhesion strength and the cohesion strength of the FRP-to-steel bonded joints (and thus the properties of the adhesive) and the interlaminar strength of CFRP plates which is a material property of CFRP. It is easy to understand why specimens E with CFRP failure had the highest ultimate load among all the specimens as the stresses developed in the CFRP plates were the highest in specimens E. For specimens B, the cohesion strength was lower than the adhesion strength, but for specimens C and D, the adhesion strength and the cohesion strength were almost the same. The load required to cause debonding failure was less than that to cause CFRP failure for specimens with these three adhesives. For specimens A, adhesion failure occurred but this may be attributed to poor bonding caused by the low viscosity of the adhesive, as explained in Section 2. It is thus difficult to draw firm conclusions for this adhesive. For the three specimens of the same adhesive, it may be noted that the ultimate loads differ significantly (Table 4) and the specimen with a lower ultimate load was found to fail in a more unsymmetrical manner than other specimens.

Table 4. Results of end bearing tests on CFRP-strengthened RHS tubes

Adhesive	Specimen	Failure mode <sup>#</sup>	Ultimate load, $P_{\text{cfRP}}$ , (kN)	Deflection at ultimate load, $\Delta_{\text{cfRP}}$ (mm)	$P_{\text{cfRP}}/P^*$	$\Delta_{\text{cfRP}}/\Delta^*$	Average $P_{\text{cfRP}}/P$	Average $\Delta_{\text{cfRP}}/\Delta$
A	A-I	A	20.69	2.02	1.09	1.107	1.15	0.80
	A-II	A	21.88	0.49	1.15	0.268		
	A-III	A	22.76	1.88	1.20	1.030		
B	B-I	C	26.91	0.79	1.42	0.434	1.43	0.52
	B-II	C	26.21	1.19	1.38	0.653		
	B-III	C	28.05	0.87	1.48	0.479		
C	C-I	A+C	28.98	1.33	1.53	0.729	1.48	0.67
	C-II	A+C	27.14	1.19	1.43	0.652		
	C-III	A+C	27.82	1.13	1.47	0.622		
D	D-I	A+ C	41.23	1.36	2.17	0.744	2.03	0.70
	D-II	A+ C	38.64	1.28	2.04	0.703		
	D-III	A+C	35.64	1.19	1.88	0.650		
E	E-I	I	42.77	1.53	2.26	0.840	2.37	0.85
	E-II	I	44.84	1.89	2.36	1.037		
	E-III	I	47.37	1.22	2.50	0.670		

\*  $P$  = ultimate web crippling load of the bare steel tube

$\Delta$  = deflection at the ultimate load of the bare steel tube

<sup>#</sup> A = Adhesion failure; C = Cohesion failure; I = Interlaminar failure of CFRP plates

Although specimens C and specimens D failed in the same mode (i.e. combined adhesion and cohesion failure), their ultimate loads are significantly different. Specimens C achieved a 48% ultimate load enhancement on average over that of the bare RHS tube while the corresponding value for specimens D is 103%. The elastic modulus and tensile strength of adhesive C are, however, much higher than those of adhesive D (see Table 3). Adhesive D is superior to adhesive C only in the ultimate tensile strain. The ultimate tensile strain of the former ( $=0.0151$ ) is approximately twice that of the latter ( $=0.0075$ ). Noting

that adhesive E which has the largest ultimate tensile strain led to the highest ultimate load, it may be concluded that the ultimate load of a CFRP-strengthened RHS tube depends much more on the ultimate tensile strain rather than the tensile strength of the adhesive. Based on existing research on FRP-plated beams (e.g. study by Smith and Teng 2002), the interfacial stresses near the plate ends reduce significantly with the elastic modulus of the adhesive. In addition, the nonlinear stress-strain behavior of adhesives D and E means that significant stress redistributions near the plate ends are possible. The better performance delivered by the adhesives D and E is believed to be the result of these two factors.

#### 4. CONCLUSIONS

This paper has presented the results of a series of end bearing tests on CFRP-strengthened RHS tubes, where five different commercially available adhesives were used to bond CFRP plates to RHS tubes. The test results showed that the adhesive properties have a strong effect on the behaviour of such CFRP-strengthened RHS tubes. Four different failure modes were observed in the tests: (1) adhesion failure; (2) cohesion failure; (3) combined adhesion and cohesion failure; (4) interlaminar failure of CFRP plates. These tests also revealed that an adhesive with a larger ultimate tensile strain leads to a greater ultimate load. In particular, adhesives D and E showed the best performance in terms of the ultimate load enhancement. In terms of gaining a better understanding of the various debonding failure modes, further research on the effect of surface characteristics on debonding failure is urgently needed.

#### ACKNOWLEDGMENTS

The authors are grateful for the financial support from The Hong Kong Polytechnic University and the Australian Research Council through its Linkage International Award Scheme.

#### REFERENCES

- Packer, J.A. (1984), "Web crippling of rectangular hollow sections", *Journal of Structural Engineering*, ASCE, 110(10), 2357-2373.
- Packer, J.A. (1987), "Review of American RHS web crippling provision", *Journal of Structural Engineering*, ASCE, 113(12), 2508-2513.
- Schnerch, D. (2005), *Strengthening of steel structures with high modulus carbon fiber reinforced polymer (CFRP) materials*, PhD dissertation, North Carolina State University, Raleigh (NC).
- Smith, S.T. and Teng, J.G. (2001), "Interfacial stresses in plated beams", *Engineering Structures*, 23(7), 857-871.
- Smith, S.T. and Teng, J.G. (2002), "FRP-strengthened RC beams-I: review of debonding strength models", *Engineering Structures*, 24(4), 385-95.
- Teng, J.G., Zhang, J.W. and Smith, S.T. (2002). "Interfacial stresses in reinforced concrete beams bonded with a soffit plate: a finite element study", *Construction and Building Materials*, Vol. 16, pp. 1-14.
- Yuan, H., Teng, J.G., Seracino, R., Wu, Z.S. and Yao, J. (2004). "Full-range behavior of FRP-to-concrete bonded joints", *Engineering Structures*, 26(5), 553-565.
- Zhao, X.L., Fernando, D. and Al-Mahaidi, R. (2006), "CFRP strengthened RHS subjected to transverse end bearing force", *Engineering Structures*, 28(11), 1555-1565.
- Zhao, X.L. and Hancock, G.J. (1992), "Square and rectangular hollow sections subject to combined actions", *Journal Structural Engineering*, ASCE, 118(3), 648-668.
- Zhao, X.L. and Hancock, G.J. (1995), "Square and rectangular hollow sections under transverse end bearing force", *Journal of Structural Engineering*, ASCE, 121(9), 1323-1329.
- Zhao, X.L. and Zhang, L. (2007). "State-of-the-art review on FRP strengthened steel structures", *Engineering Structures*, 29(8), 1808-1823.
- Zhou, F. (2006), *Web Crippling of Cold-formed Stainless Steel Tubular Sections*, PhD thesis, The University of Hong Kong, Hong Kong SAR.